Materials Letters 236 (2019) 460–464

Contents lists available at ScienceDirect

Materials Letters

journal homepage: www.elsevier.com/locate/mlblue

Direct and seedless growth of Nickel Oxide nanosheet architectures on ITO using a novel solution immersion method

M.A.R. Abdullah [a], M.H. Mamat [a,b,*], A.S. Ismail [a], M.F. Malek [a,b], A.B. Suriani [c], M.K. Ahmad [d], I.B. Shameem Banu [e], R. Amiruddin [e], M. Rusop [a,b]

[a] NANO-ElecTronic Centre (NET), Faculty of Electrical Engineering, Universiti Teknologi MARA (UiTM), 40450 Shah Alam, Selangor, Malaysia
[b] NANO-SciTech Centre (NST), Institute of Science (IOS), Universiti Teknologi MARA (UiTM), 40450 Shah Alam, Selangor, Malaysia
[c] Nanotechnology Research Centre, Faculty of Science and Mathematics, Universiti Pendidikan Sultan Idris (UPSI), 35900 Tanjung Malim, Perak, Malaysia
[d] Microelectronic and Nanotechnology – Shamsuddin Research Centre (MiNT-SRC), Faculty of Electrical and Electronic Engineering, Universiti Tun Hussein Onn Malaysia (UTHM), Batu Pahat, Johor, Malaysia
[e] Department of Physics, B.S. Abdur Rahman Crescent Institute of Science & Technology, Vandalur, Chennai 600 048, India

ARTICLE INFO

Article history:
Received 5 September 2018
Received in revised form 26 October 2018
Accepted 29 October 2018
Available online 29 October 2018

Keywords:
Semiconductors
NiO nanosheets
Sol–gel preparation
Solution immersion method
Structural and optical properties
Liquid ethanol sensor

ABSTRACT

Nickel Oxide (NiO) nanosheet architecture films were synthesized using solution immersion method on indium tin oxide (ITO)-coated glass at different growth times. The X-ray diffraction patterns and Raman spectra reveal that crystalline NiO films were grown on ITO glass. The microscopy images exhibit the presence of 10 nm-width nanosheet architectures. The thickness of NiO nanosheet array films increases from 0.78 μm to 2.50 μm, when the growth time increases from 1 h to 3 h. The estimated energy bandgap for the prepared NiO nansosheets ranges from 3.55 to 3.62 eV. The prepared NiO nanosheet architecture films has good optical transmittance in the visible region. In this work, the synthesized NiO nanosheet arrays have high potential application for liquid ethanol sensor based on a good sensing response at room temperature.

1. Introduction

Nickel Oxide (NiO) is a wide band gap semiconductor material with energy of 3.6–4.0 eV [1]. Particularly in nanostructures, NiO has attracted many interests for investigation in field of magnetic material, photocatalysts, and sensor due to outstanding physical and chemical properties. Up to date, several methods have been used to prepare NiO nanostructures including sputtering, spray-pyrolysis, and hydrothermal.

Herein, we proposed a novel approach to prepare NiO nanosheet array films using solution immersion method in water bath via Schott bottle for liquid ethanol sensing applications. This technique provides the direct growth of NiO nanosheet film on the ITO substrate without NiO seed layer. Earlier reports showed that the growth of NiO nanosheet on the substrate requires NiO seed layer [2–4]. For example, Xia et al. synthesized NiO nanosheet arrays on NiO film-coated glass substrate using hydrothermal method [2]. The NiO film, which act as the seed layer, was prepared using sol–gel spin-coating technique at 1000–2000 rpm for 30 s. They acquired the nanosheet arrays with the width of 200–400 nm after hydrothermal process for 2 h at 90 °C. Luan et al. synthesized three-dimensional porous nitrogen-doped NiO nanosheet on spin-coated NiO seed layer-coated Si/SiO_2 wafer using dip growth process [3]. The NiO seed layer was spin-coated at 4000 rpm for 30 s. After the dip-growth process at 90 °C for 2 h, they obtained the NiO nanosheet arrays with the width of 20–30 nm. Hoa et al. synthesized NiO nanosheet on a zinc oxide (ZnO) nanorod array-coated SiO_2/Si wafer using hydrothermal process [4]. Prior to the NiO nanosheet growth, NiO seed layer was deposited on the ZnO nanorod arrays using spin-coating process. They observed 20 nm-width NiO nanosheets were grown on ZnO nanorod after hydrothermal process at 90 °C for 30 min. Wu et al. synthesized iron doped NiO mesoporous nanosheet arrays on Ni foam using autoclave solvothermal method [5]. The process was conducted at 120 °C for 8 h to yield 10 nm-width NiO nanosheet arrays on Ni foam. However, the direct growth of NiO on ITO glass substrate is very promising for electronic device applications since the ITO glass is widely used as transparent conducting electrode (TCE) in the electronic industries. To our knowledge, there are only few reports on the fabrication of NiO nanosheet array films using solution immersion approach in the water bath. Furthermore, the liquid ethanol sensing performance

* Corresponding author.
E-mail address: mhmamat@salam.uitm.edu.my (M.H. Mamat).

https://doi.org/10.1016/j.matlet.2018.10.163
0167-577X/

based on NiO nanosheet architectures has been rarely reported. This technique shows effective, reliable, and convenient approach for the growth of NiO nanosheet.

2. Experimental

In this experiment, 0.1 M nickel nitrate hexahydrate ($Ni(NO_3)_2 \cdot 6H_2O$) and 0.1 M hexamethylenetetramine (HMT, $C_6H_{12}N_4$) were mixed into a beaker filled with 300 ml deionized (DI) water. Then, the solution was sonicated for 30 min using an ultrasonic water-bath (Hwasin Technology Powersonic 405, 40 kHz). Next, the solution was poured into Schott bottles. Commercially purchased indium-doped tin oxide (ITO, sheet resistance value: 15 Ω·cm, size: 2 cm × 2 cm) coated glass substrates were placed at the bottom of the bottle. The bottles were closed tightly and immersed in water-bath at 95 °C for 1 h, 2 h, and 3 h to yield different thicknesses. The experimental setup is shown in Fig. 1(a). After immersion process,

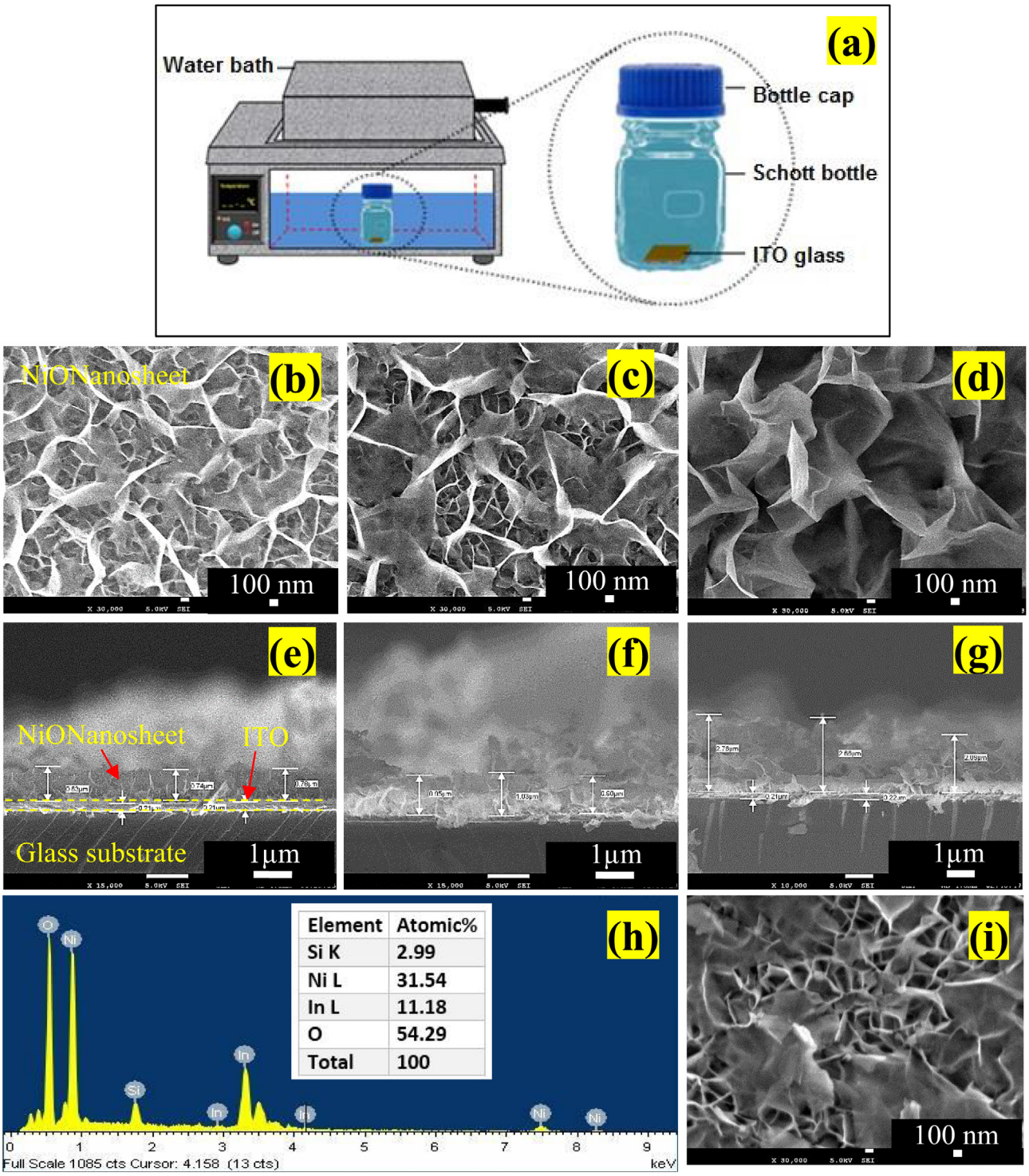

Fig. 1. (a) Experimental setup for preparing NiO nanosheet arrays in water bath with Schott bottle. The FESEM images of NiO nanosheets array films grown at different times of (b) 1 h, (c) 2 h, and (d) 3 h at magnification of 30,000×. The cross-section of synthesized NiO nanosheets thin film grown at (e) 1 h, (f) 2 h and (g) 3 h. (h) The EDS spectrum of NiO nanosheets arrays. (i) NiO nanosheet arrays grown on bare glass substrate.

the samples were rinsed with DI water and baked at 150 °C for 10 min. Then, the samples were annealed at 400 °C for 1 h to improve the crystallinity of the films.

The morphologies and structural properties of prepared NiO samples were examined using field-emission scanning electron microscopy (FESEM, JEOL JSM-7600F), X-ray diffraction (XRD, PANalytical X'pert PRO and micro-Raman spectroscopy (Horiba Jobin Yvon-79 DU420A-OE-325, 514 nm Ar laser). The elemental analysis was conducted using energy dispersive X-ray spectroscopy (EDS, INCA). The optical properties of the samples were characterized by ultraviolet–visible (UV–Vis) spectrophotometry (Varian Cary 5000). The ethanol liquid responses of the samples was investigated using current–voltage measurement system (Keithley 2400) at room temperature with a bias voltage of 1 V. For ethanol sensing measurement, a drop of liquid ethanol (0.05 ml) was applied directly onto the films and the current signal was measured.

3. Results and discussion

The surface morphologies of the samples at different growth times are depicted in Fig. 2(b)–(d), which show that the synthesized samples have nanosheet array architectures. The results also indicate that the deposited NiO nanosheets are uniformly grown on the ITO glass with porous morphologies and forms stacked nanosheet structures. As the immersion time increases, the growth of nanosheet was enhanced. Interestingly, the width of each individual nanosheet remain unchanged at approximately 10 nm regardless the growth time. The width of the synthesized nanosheet is smaller than the width of the nanosheet grown on the NiO seed layer in the previous reports [2–4]. Fig. 2(e)–(g) shows the cross-sectional images of NiO nanosheet films at growth time of 1 h, 2 h, and 3 h, which have an average thickness of 0.78 μm, 0.96 μm, and 2.50 μm, respectively. The EDS analysis shown in Fig. 2(h) confirms the presence of Ni and O elements

substrate.

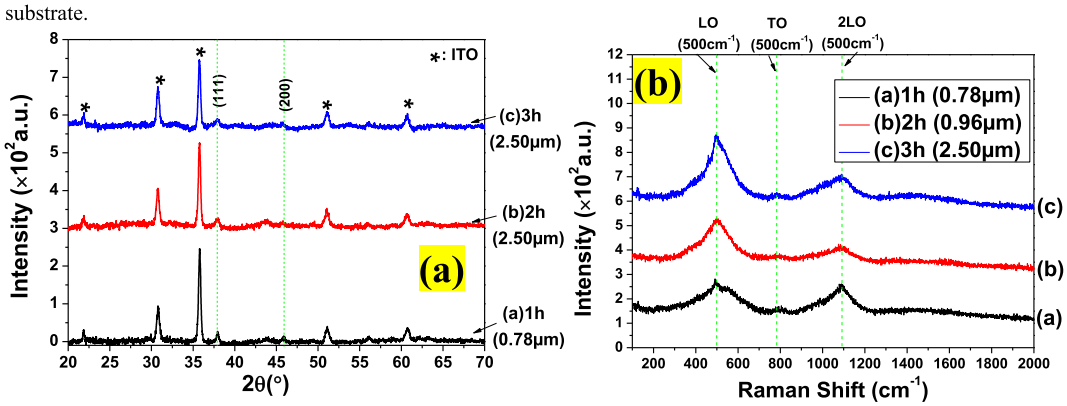

Fig. 2. (a) XRD pattern and (b) Raman spectra of NiO nanosheet films grown at different times.

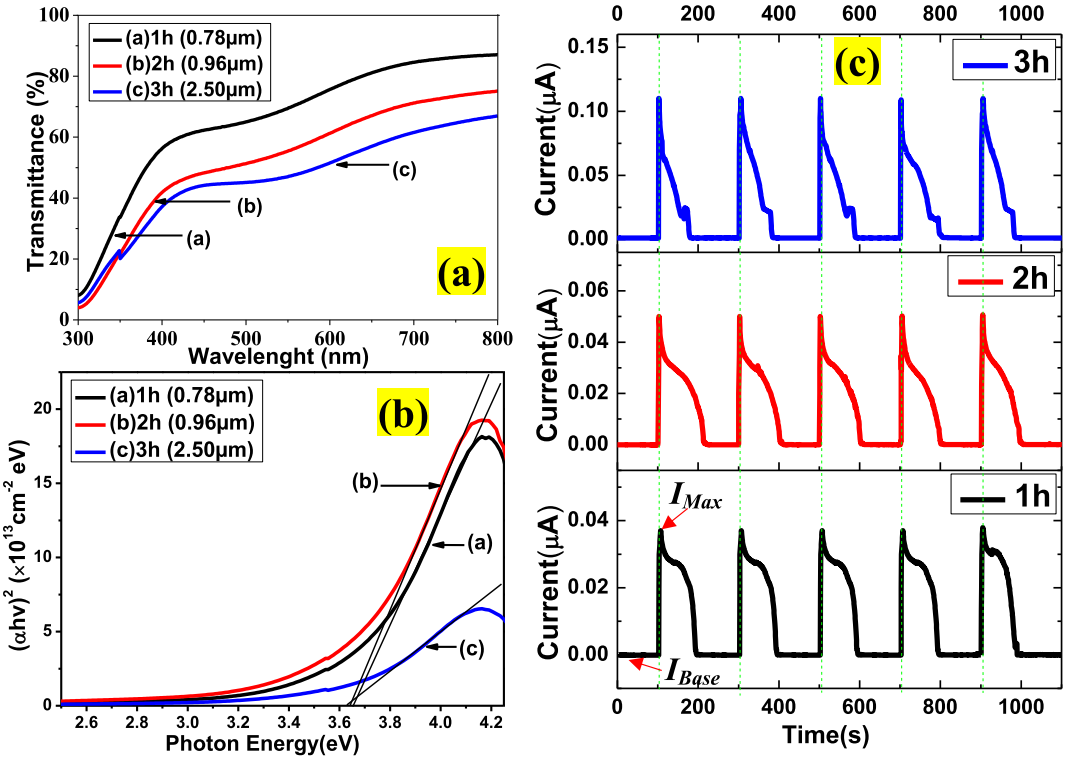

Fig. 3. (a) UV–Vis transmittance spectra, (b) Tauc's plot, and (c) room temperature liquid ethanol response of the NiO nanosheet array films at different growth times.

Table 1
Comparison of the ethanol (vapor/gas and liquid) sensing performance between the NiO nanosheet film and previously reported results.

Sensing material	State (concentration)	Temperature (°C)	Sensitivity	Ref.
NiO nanosheet (powder)	Gas (200 ppm)	200	3.11	[10]
1.5% Fe_2O_3/NiO nanosheets	Gas (1000 ppm)	255	4×10^2	[11]
NiO/ZnO microspheres	Gas (175 ppm)	260	90	[12]
ZnO	Liquid (3600 ppm)	RT	1.43	[13]
ZnO/SnO_2 spheres	Gas (50 ppm)	240	34.8	[14]
NiO nanosheet (film)	Liquid (0.05 ml)	RT	1.66×10^3	

along with In and Si, which originates from the substrate. Fig. 2(i) depicts the morphological structure of grown film on a bare glass substrate deposited for 1 h. Interestingly, the NiO nanosheet film was observed to grow on the bare glass substrate. However, the adhesion of the film on the glass substrate is not as strong as the film on the ITO glass and the film can easily scratched and removed. This condition might be due to lattice mismatch between NiO film and amorphous glass is higher than that of the ITO glass, which forms a weak bonding between the film and glass substrate.

The formation of NiO nanosheets can be described as follows. First, HMT decomposes into formaldehyde and ammonia. The ammonia reacts with water to release ammonium ion and hydroxide ion in the process. Thus, it can be suggested that the HMT act as a pH buffer, which supplies hydroxide ion through these reactions. The main chemical reactions are described as:

$$C_6H_{12}N_4 + H_2O \rightarrow 6CH_2O \rightarrow 4NH_3, \quad (1)$$

$$NH_3 + H_2O \rightarrow NH_4^+ + OH^-, \quad (2)$$

$$Ni^{2+} + 2OH^- \rightarrow NiO + H_2O \quad or \quad Ni^{2+} + 2OH^- \rightarrow Ni(OH)_2 \rightarrow NiO + H_2O \quad (3)$$

During the growth of NiO nanosheets (Eq. (2)), the concentration of OH^- anions become very dominant. With the sufficient quantity of OH^- ions, it achieves supersaturation; subsequently, Ni^{2+} ions react with OH^- ions to form NiO nuclei on the ITO surface, thus initiating the growth of NiO nanosheets (Eq. (3)). Successively, under the supply of thermal energy, the nuclei expands to form networks of interconnected nanosheets.

The formation of crystalline NiO phase for all samples were confirmed from the XRD pattern as shown in Fig. 2(a). The NiO characteristic peaks were observed at 2θ value of 37.9° and 45.9°, which corresponds to the crystal planes of (1 1 1) and (2 0 0), respectively [6]. All these peaks are indexed to crystalline cubic structure of NiO, which matches well with NiO standard pattern (JCPDS NO. 47-1049). The structural analysis based on XRD data is presented in supplementary material. The obtained XRD pattern is comparable to the XRD pattern of NiO on the seed layer as reported by other researchers [2–5].

The Raman spectra of NiO nanosheet architectures at different growth times are shown in Fig. 2(b). There are two prominent peaks observed in the spectra located at approximately 500 cm^{-1} and 1090 cm^{-1}, corresponding to longitudinal optical (LO) and 2LO phonon modes of NiO, respectively. A weak peak at approximately 785 cm^{-1} was also observed, which indicates the presence of NiO two-transverse optical (2TO) vibration mode. This finding satisfies the characteristics of cubic NiO, which also matches with the XRD results.

The optical transmittance spectra of the NiO nanosheet in a range of 300–800 nm are shown in Fig. 3(a). The average transmittance of NiO nanosheet architectures in the visible region are 75%, 61%, and 53% at the growth time of 1 h, 2 h, and 3 h, respectively. The reduced transmittance with the growth time might be associated with the increases of thickness and scattering effect in the porous NiO nanosheet architectures [7]. The optical band gap energy (E_g) of the films were examined from the Tauc's plot of NiO nanosheets shown in Fig. 3(b), which was calculated using Tauc's relation below:

$$\alpha h\nu = B(h\nu - E_g)^{1/2}, \quad (4)$$

where α is the absorption coefficient, $h\nu$ is the photon energy, B is a constant, and E_g is the bandgap energy. The values of optical band gap energy of the film were obtained by extrapolation of the linear region. The energy band gap values for samples at the growth time of 1 h, 2 h, and 3 h are 3.66 eV, 3.64 eV, and 3.62 eV, respectively [8]. These narrowing band gap might be due to the expansion of lattice size (see supplementary material) [9].

Fig. 3(c) shows the liquid ethanol response characteristics of NiO nanosheets for different growth times. The highest current values upon liquid ethanol exposure was obtained for NiO at growth time of 3 h, follows by 2 h and 1 h. From these results, the sensitivity, which is defined as a ratio of current values upon liquid ethanol exposure, I_{Max} over initial current value (before ethanol exposure), I_{Base} was calculated. The sensitivity values were calculated to be 2.23×10^2, 3.82×10^2, and 1.66×10^3 for NiO nanosheet at growth time of 1 h, 2 h, and 3 h, respectively. The acquired response times of the samples at the growth time of 1 h, 2 h, and 3 h are are 2.8 s, 2.6 s, and 0.6 s, respectively. All films show good response to the liquid ethanol due to the porous nanosheet architectures, which provide very large surface area for ethanol interaction. The porous channels inside NiO nanosheet films also improve with the increase in the thickness, which provides more sites for ethanol sensing reaction and thus enhances the ethanol response. The sensing mechanism is discussed in supplementary material. Table 1 shows the sensing performance of previous reports using various metal oxide structures for ethanol vapor/gas and liquid ethanol detections. Based on this table, the synthesized NiO nanosheet film shows a promising result for liquid ethanol sensing.

4. Conclusions

A direct growth of NiO nanosheet architectures was successfully achieved on ITO glass using a novel approach of solution immersion method at different growth times without NiO seed layer. The uniform films consisting of dense and porous NiO nanosheets were observed from morphological analysis. The thickness of the films increase with the growth time. The NiO nanosheet array-based sensors demonstrate high sensitivity to liquid ethanol with values in the range of 2.23×10^2 to 1.66×10^3. The good response to liquid ethanol might be due to the high surface area of NiO nanosheet architectures. In conclusion, grown NiO nanosheet arrays are a promising material for liquid ethanol sensing.

Acknowledgements

This research was supported by the ASEAN-India Research & Training Fellowship (IMRC/AISTDF/R&D/P-1/2017). This work was also supported by REI grant (600-IRMI/REI 5/3 (017/2018)). The authors acknowledged the Faculty of Electrical Engineering and

Institute of Research Management and Innovation (IRMI) of UiTM for their financial support.

Appendix A. Supplementary data

Supplementary data to this article can be found online at https://doi.org/10.1016/j.matlet.2018.10.163.

References

[1] R. Miao, W. Zeng, Hydrothermal synthesis of flake-flower NiO architectures: structure, growth and gas-sensing properties, Mater. Lett. 171 (2016) 200–203.
[2] Q.X. Xia, K.S. Hui, K.N. Hui, D.H. Hwang, S.K. Lee, W. Zhou, et al., A facile synthesis method of hierarchically porous NiO nanosheets, Mater. Lett. 69 (2012) 69–71.
[3] V. Luan, H. Tien, S. Hur, J. Han, W. Lee, Three-dimensional porous nitrogen-doped NiO nanostructures as highly sensitive NO_2 sensors, Nanomaterials 7 (2017) 313.
[4] L.T. Hoa, H.N. Tien, S.H. Hur, Fabrication of novel 2D NiO nanosheet branched on 1D-ZnO nanorod arrays for gas sensor application, J. Nanomater. 2014 (2014) 6.
[5] Z. Wu, Z. Zou, J. Huang, F. Gao, Fe-doped NiO mesoporous nanosheets array for highly efficient overall water splitting, J. Catal. 358 (2018) 243–252.
[6] R. Miao, W. Zeng, Q. Gao, SDS-assisted hydrothermal synthesis of NiO flake-flower architectures with enhanced gas-sensing properties, Appl. Surf. Sci. 384 (2016) 304–310.
[7] M. Predanocy, I. Hotový, M. Čaplovičová, Structural, optical and electrical properties of sputtered NiO thin films for gas detection, Appl. Surf. Sci. 395 (2017) 208–213.
[8] M.M. Gomaa, G.R. Yazdi, S. Schmidt, M. Boshta, V. Khranovskyy, F. Eriksson, et al., Effect of precursor solutions on the structural and optical properties of sprayed NiO thin films, Mater. Sci. Semicond. Process. 64 (2017) 32–38.
[9] R. Ghosh, D. Basak, S. Fujihara, Effect of substrate-induced strain on the structural, electrical, and optical properties of polycrystalline ZnO thin films, J. Appl. Phys. 96 (2004) 2689–2692.
[10] C. Zhao, J. Fu, Z. Zhang, E. Xie, Enhanced ethanol sensing performance of porous ultrathin NiO nanosheets with neck-connected networks, RSC Adv. 3 (2013) 4018–4023.
[11] W. Tan, J. Tan, L. Fan, Z. Yu, J. Qian, X. Huang, Fe_2O_3-loaded NiO nanosheets for fast response/recovery and high response gas sensor, Sens. Actuator B-Chem. 256 (2018) 282–293.
[12] L. Zhu, W. Zeng, J. Yang, Y. Li, Fabrication of hierarchical hollow NiO/ZnO microspheres for ethanol sensing property, Mater. Lett. 230 (2018) 297–299.
[13] Y.-M. Lee, C.-M. Huang, H.-W. Chen, H.-W. Yang, Low temperature solution-processed ZnO nanorod arrays with application to liquid ethanol sensors, Sens. Actuator A-Phys. 189 (2013) 307–312.
[14] J. Liu, T. Wang, B. Wang, P. Sun, Q. Yang, X. Liang, et al., Highly sensitive and low detection limit of ethanol gas sensor based on hollow ZnO/SnO_2 spheres composite material, Sens. Actuator B-Chem. 245 (2017) 551–559.